Tetrahedron: *Asymmetry* 19 (2008) 1660–1669

Contents lists available at ScienceDirect

Tetrahedron: *Asymmetry*

journal homepage: www.elsevier.com/locate/tetasy

A DFT study of 1,3-dipolar cycloaddition reactions of 5-membered cyclic nitrones with α,β-unsaturated lactones and with cyclic vinyl ethers: Part 1

Sebastian Stecko [a], Konrad Paśniczek [a], Carine Michel [b], Anne Milet [b], Serge Pérez [c], Marek Chmielewski [a,*]

[a] *Institute of Organic Chemistry of the Polish Academy of Sciences, 01-224 Warsaw, Poland*
[b] *Département de Chimie Moléculaire, Université Joseph Fourier, BP53, 38041 Grenoble, France*
[c] *Centre de Recherches sur les Macromolécules Végétales, CNRS, BP53, 38041 Grenoble, France*

ARTICLE INFO

Article history:
Received 28 April 2008
Accepted 4 July 2008
Available online 27 July 2008

ABSTRACT

The 1,3-dipolar cycloaddition of cyclic nitrones with electron-poor and electron-rich cyclic dipolarophiles (α,β-unsaturated lactones and vinyl ethers) is studied. The energies of the cycloaddition reactions have been investigated through molecular orbital calculations at the B3LYP/6-31+G(d) level theory. Different reaction channels and reactants approaches, effective in regio- and stereochemical preferences are discussed. The results were compared with experimental data to find a good agreement.

1. Introduction

The 1,3-dipolar cycloaddition reactions (1,3-DC) represent a useful tool for the construction of both heterocyclic and carbocyclic rings.[1–3] Reactions between nitrones and alkenes leading to isoxazolidine rings are among the best known processes of this kind.[1] The formation of functionalized isoxazolidines and then, after hydrogenolysis of the N–O bond, β-amino alcohols plays an important role in the synthesis of nitrogen-containing compounds.[4–6]

The general usefulness of 1,3-dipolar cycloadditions involving nitrones in target-oriented syntheses[4–11] and our experimental observations[12,13] inspired us to study further cycloadditions involving cyclic 5-membered nitrones (e.g. **N**) and unsaturated γ- and δ-lactones (e.g. **L1** and **L2**) via computational methods. We decided to extend these theoretical calculations to model 1,3-DC involving cyclic nitrones and unsaturated cyclic ethers—dihydrofuran **E1** and dihydropyran **E2**, as well.

In contrast to the Diels–Alder reaction which has received a great deal of theoretical attention,[14–16] there are not many computational studies of 1,3-DCs of nitrones to multiple carbon–carbon bonds.[17–30] Ten years ago, Tanaka et al.[17] examined the 1,3-DC of 3,4-dihydroisoquinoline *N*-oxide to methyl 2-butenoate. The authors proposed a concerted mechanism with a nonsymmetric transition state in which the C–O bond is formed to a greater degree than the C–C one. The exclusive formation of the *endo*-adduct can be attributed to the stabilizing secondary orbital interactions of the ester carbonyl group with both the phenyl ring and the HOMO lobe on the nitrogen atom. Houk et al.[21] have performed ab initio calculations on the 1,3-DC of a simple hypothetical model nitrone **1** to dipolarophiles containing electron-releasing substituents. Once again, the *endo*-product is kinetically favored owing to stabilizing secondary orbital interactions. It should be noted, however, that the simplest nitrone may occur rather as formaldoxime, and a formal 1,2-hydrogen shift to form the nitrone structure requires the high energy of activation; consequently, the cycloaddition may have a stepwise mechanism.[23]

Pranata and Manguson[24] have studied the regioselectivity of nitrone cycloadditions. While in the 1,3-DCs between **1** and electron-rich alkenes, the *ortho*-regioisomers were predicted to be more favorable than the *meta* ones (see Schemes 2 and 3 for regiochemical description), in the case of the cycloaddition to electron-poor alkenes, calculations predicted a lack of regioselectivity. The reaction of **1** and nitroethylene has been investigated by Cossío et al.[26] The asynchronicity in the bond formation process in the two regioisomeric approaches of nitroethylene to the nitrone is controlled by the electron-poor dipolarophile; the bond formation at the β-position of the alkene has been found to be more advanced than that at the α-position. Their calculations predicted an *endo*-stereoselectivity and *meta*-regioselectivity. The latter has not been confirmed by experimental data.[26] The authors suggested that regioselectivity of these reactions cannot be predicted by means of simple electronic arguments, but also steric and polar effects must be taken into consideration to account for both the regio- and the stereochemical outcome.

Domingo[27a] has studied the 1,3-DC of nitrone **2** to the *tert*-butyl vinyl ether. B3LYP/6-31G* calculations predicted an *exo*-stereoselectivity with an *ortho*-regioselectivity, which are in agreement with experimental data.[27a] The *exo*-stereoselectivity has been assigned, since in the case of the *endo*-approach a steric hindrance is progressively developed between the phenyl group at the nitrogen atom and the *tert*-butyl group of the ether. Incorporation of

* Corresponding author. Tel./fax: +48 22 632 66 81.
E-mail address: chmiel@icho.edu.pl (M. Chmielewski).

0957-4166/$ - see front matter © 2008 Elsevier Ltd. All rights reserved.
doi:10.1016/j.tetasy.2008.07.008

solvent effects increased the activation energies and decreased the exothermic result of the process because of a greater solvatation of a polar nitrone than that of the TSs and cycloadducts.[25,26] Solvents also cause a higher stabilization of the *endo*-TS and, as a consequence, a slight decrease in the stereoselectivity.

The 1,3-DC of the cyclic nitrone **3** to methyl propiolate and acrylonitrile has been studied by Marco and Domingo.[27b] For the reaction with methyl propiolate, DFT calculations predicted the experimentally observed *meta*-regioselectivity. However, for the reaction with acylonitrile, the predicted regioselectivity has been found to depend on the computational level used. Further calculations indicated the *exo*-approach to be energetically favored for the latter dipolarophile (in agreement with experimental findings) due to the steric repulsion of the nitrile function and methyl substituents of the nitrone that progressively develops in the alternative *endo*-approach.

Merino et al.[28] have studied the 1,3-DCs of both electron-poor and electron-rich alkenes to the D-glyceraldehyde nitrone **5**,[28b] glyoxylic nitrone **6**,[28c] and C-heteroaryl nitrones **7**.[28d] Taking into consideration conformational lability of the nitrones, the predictions thus obtained are in good agreement with experimental findings.

Langlois et al.[29] have performed calculations of frontier molecular orbital energies and coefficients of the oxazoline type nitrone **4** and electron-poor alkenes using RHF/AM1 level. These studies confirmed experimentally observed *endo*-selectivity. The authors explained such a preference by a second-order orbital interaction between the electron-withdrawing group of the olefin and the *endo*-ring oxygen atom of the nitrone molecule.

The competition of concerted versus stepwise mechanism in 1,3-DC of nitrone **1** to ethene, cyclobutadiene, and benzocyclobutadiene was studied by Gandolfi et al.[31a] R(U)B3LYP/6-31G* calculations demonstrated that in case of ethene and benzocyclobutadiene product formation should take place via the concerted cycloaddition path. In the case of the reaction of nitrone **1** with reactive antiaromatic cyclobutadiene, which may promote a stepwise diradical pathway, R(U)B3LYP/6-31G* calculations suggest that it is a borderline case in which a stepwise process can compete with concerted mechanism.[31a]

Gandolfi[31b] also studied the 1,3-DC of nitrone **1** with vinylboranes. The performed calculations showed that vinylboranes may undergo very fast [3+2] cycloaddition to nitrones resulting in a single *endo*-adduct. It was also pointed out that the boronyl substituent is intimately involved in the reaction mechanism via very strong B···O interactions that are able to produce very low energy barriers, regioselectively, and to complete *endo*-selectivity, in a sort of effective and selective intramolecular catalysis.[31b]

As a part of our research on the application of 1,3-DC reactions in the synthesis of polyhydroxylated alkaloids,[12] we investigated reactions between cyclic 5-membered nitrones with 5- and 6-membered lactones.[13,32,33] The reactions involving 6-membered lactones showed the formation of *exo*-adducts exclusively in high diastereoselectivity.[12a,13b,c] Conversely, 5-membered lactones react with lower diastereoselectivity affording mixture of products; in this case we have observed formation of *endo*-adducts, as well.[32,33] Similar results have been reported by Font et al.[34] for simple nitrone **N** and lactones **L1**/**L2** (Scheme 1). Moreover, it was found that the stereochemical pathway of cycloadditions involving γ-lactones is more complicated due to reversibility of the reactions, which has not been observed for δ-lactones.[33]

A few years ago, in a paper from the University of Florence and our laboratory,[35] cycloadditions of cyclic nitrones to glycals were investigated. In all cases, the formation of *exo*-adducts has been observed, exclusively. For these simple cyclic dipolarophiles Kakisawa et al.[36] have observed high *exo*-selectivity, as well (Scheme 1).

Herein, we report preliminary part of our theoretical studies on 1,3-DC reactions. This is the first attempt to analyze reactions between cyclic nitrones and cyclic dipolarophiles. As models we chose cycloadditions investigated by Font[34] and Kakisawa[36] involving simple nitrone **N**, lactones **L1**/**L2**, and ethers **E1**/**E2**. Our theoretical studies represent a good starting point for the analysis of the more complicated cases of 1,3-DCs including asymmetric induction with chiral cyclic nitrones and chiral lactones or ethers. This would provide interesting examples of simple diastereoselective cycloadditions, or double asymmetric inductions, where the chirality elements of each reactant may influence the stereoselectivity either in concert or in opposition, matched and mismatched pairs.

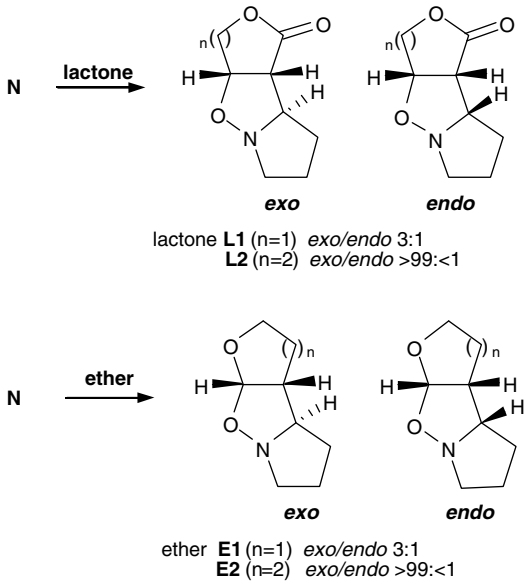

Scheme 1. The 1,3-DC of nitrone **N** to lactones **L1** and **L2**[34] and ethers **E1** and **E2**.[36]

2. Computational methods and computational models

All calculations were carried out with GAUSSIAN 03 suite of software.[37] Geometry optimizations of the stationary points (reactants, oriented complexes, transition structures, and products) were carried out using DFT methods at the B3LYP/6-31+G(d) level theory.[38] The stationary points were characterized by frequency calculations in order to verify that minima and transition structures (TSs) have zero and one imaginary frequency, respectively. The optimizations were carried out using the Berny analytical gradient optimization method.[39] The electronic structures of the critical points were studied by the natural bond orbital (NBO) method.[40] The intrinsic reaction coordinates (IRC)[41] were also calculated to analyze the mechanism in detail for all the transition structures obtained.

As a computational model, we used the simplest cyclic 5-membered nitrone **N** to investigate regio- and diastereoselectivity for its reaction with lactones **L1** and **L2** and cyclic ethers **E1** and **E2**. We considered two reaction channels, ortho and meta, corresponding to two possible substitutions of isoxazolidines. For both channels, *exo*- and *endo*-approaches were studied. Consequently, four transition states leading to four possible cycloadducts were located for each nitrone–lactone or nitrone–ether pair. As an experimental reference, we used Font's[34] and Kakisawa's[36] reports (Scheme 1).

3. Results and discussion

3.1. Analysis of FMO interactions. Prediction of regioselectivity

Figure 1 presents the geometry of the nitrone **N** and several important electronic and structural parameters. The N_2–O_1 and

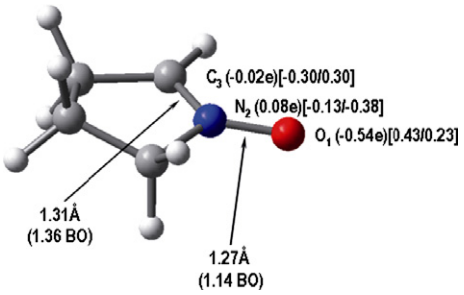

Figure 1. B3LYP/6-31+G(d) optimized geometry of nitrone **N**. Bond lengths, Wiberg bond orders (BO), natural charges, and orbital coefficients [HOMO/LUMO] for O_1, N_2, and C_3 atoms are included.

C_3–N_2 bond lengths are 1.27 and 1.31 Å, respectively (for the numbering of atoms see Chart 2). However, bond order (BO) analysis shows that the former one has more of a single bond character (1.14 BO) than the latter one (1.36 BO). This observation corresponds well with other studies on cyclic nitrones.[27b] The natural population analysis (NPA)[42] for this nitrone indicates that oxygen O_1 atom supports a negative charge (−0.54 e). A very small negative charge was also found on carbon C_3 (−0.02 e).

The frontier molecular orbital analysis for the cycloadditions studied shows that the main interactions occur between the $HOMO_{dipole}$ of **N** and the $LUMO_{dipolarophile}$ of the electron-poor alkenes, either 5- or 6-membered lactone (Fig. 2). In the case of electron-rich unsaturated ethers, the main interaction is between the $HOMO_{dipolarophile}$ of the ether and the $LUMO_{dipole}$ of the nitrone.

In general, the regioselectivity of these cycloadditions could be rationalized in terms of a more favorable FMO interactions between the largest coefficient centers of the dipole and the dipolarophile. The similar values of molecular coefficient of nitrone (at oxygen O_1 and carbon C_3 of both HOMO and LUMO, Fig. 1) as well as of LUMO of lactones and HOMO of ethers (Table 1) make such predictions difficult. It can be assumed, however, that an overlap of the O_1 orbital of the nitrone with C_4 orbital of the lactone and the C_3 orbital of the nitrone and the C_3 of the lactone should be preferred for the nitrone–lactone pair. On the other hand, for the nitrone–ether pair, an overlap of the O_1 orbital of the nitrone with the C_2 orbital of the ether as well as the C_3 orbital of the nitrone and the C_3 orbital of the ether should dominate.

Molecular density distribution for reactants confirms the above predictions. In the case of the nitrone **N**, a negative charge on both O_1 (−0.54 e) and C_3 (−0.02 e) atoms was found. The lactones **L1**/**L2** have, on average, negative charges on C_3 (−0.33 e) and C_4 (−0.19 e) atoms, whereas ethers **E1**/**E2** have positive charges on C_2 (0.13 e) atom and negative one on C_3 (−0.35 e) atom.

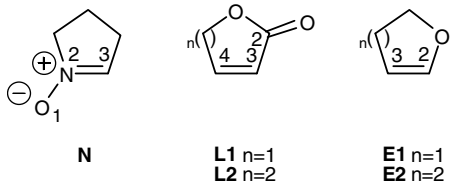

Chart 2.

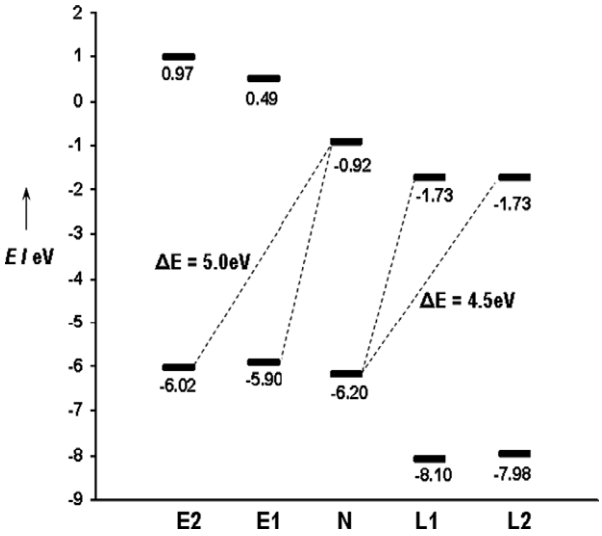

Figure 2. FMO interactions in the 1,3-DC reactions of the nitrone **N** with lactones **L1** and **L2** and ethers **E1** and **E2**.

Table 1
Molecular coefficients of dipolarophiles[a]

		C_4	C_3
L1	LUMO	0.40	−0.28
	HOMO	−0.26	−0.29
L2	LUMO	−0.39	0.26
	HOMO	0.33	0.35
		C_3	C_2
E1	LUMO	0.34	−0.39
	HOMO	−0.38	−0.27
E2	LUMO	0.17	−0.27
	HOMO	0.39	0.28

[a] For numbering of atoms see Chart 1.

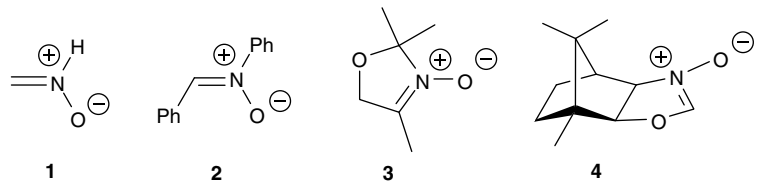

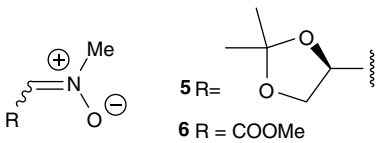

Chart 1.

In principle, the more nucleophilic center should react with the less nucleophilic one. Hence, in the reaction of **N** with **L1**/**L2** the more nucleophilic oxygen of the nitrone should attack the C_4 atom of the lactone more preferably than the C_3 one. Consequently, it provides the isomer with the nitrone oxygen atom attached to C_4 atom of the lactone and the nitrone C_3 atom attached to C_3 atom of the lactone. Conversely, in the reaction of the nitrone **N** with cyclic vinyl ethers, the formation of the isomer with the nitrone oxygen attached to the C_2 atom of the ether and consequently the nitrone C_3 atom to the C_3 atom of the ether should be observed.

The above analysis of the regioselectivity via FMO and charge distribution analysis gives the same results. For both approaches, a *meta*-regioselectivity is predicted for lactones and an *ortho*-regioselectivity for ethers. These results correlate very well with experimental data.[34,36,43]

3.2. The 1,3-DC reaction of nitrone N with lactones L1 and L2

3.2.1. Energies

The cycloaddition of the nitrone **N** with the lactone **L1** or **L2** can take place along four channels corresponding to *exo*- and *endo*-approaches of reactants in two possible regioisomeric senses: the *ortho* and *meta* pathways (see Scheme 2). For each nitrone–lactone pair, we have studied four TSs: **TS1-ex** (**TS3-ex**), **TS1-en** (**TS3-en**), **TS2-ex** (**TS4-ex**), and **TS2-en** (**TS4-en**); and four cycloadducts: **P1-ex** (**P3-ex**), **P1-en** (**P3-en**), **P2-ex** (**P4-ex**), and **P2-en** (**P4-en**).

A schematic representation of the stationary points along all reaction channels is presented in Scheme 2. Figure 3 presents the geometries of TSs corresponding to the 1,3-DC reactions involving γ- (**L1**) and δ-lactones (**L2**), respectively; Table 2 reports relative energies for the transition states of cycloadditions for both lactones. It was assumed that reactions proceeded from reactants [N+L] to cycloadducts via formation of van der Waals' molecular complexes [N···L] prior to the transition state structures.[44]

From transition structures, the related minima associated with the final cycloadducts can be obtained. All cycloaddition pathways are slightly exothermic processes in the range of −13.2 to −7.1 kcal/mol. For the process involving lactone **L1**, the *meta* cycloadducts **P1-ex** and **P1-en** are more stable than the *ortho* ones (**P2-ex** and **P2-en**). For *meta* channels, both enthalpy and free energy show that the *exo*-product **P1-ex** has a lower energy than the *endo* **P1-en**. A larger stability of the *exo*-adduct is also observed for the *ortho* channel. The same trend was noticed for the reaction involving 6-membered lactone **L2**; the **P3-ex**/**P3-en** pair displays lower energies than the **P4-ex**/**P4-en** one. However, in comparison to the reaction involving **L1**, the energy difference between both *meta*-adducts **P3-ex**/**P3-en** is lower ($\Delta\Delta H$ only 0.4 kcal/mol) than for the **P1-ex**/**P1-en** pair ($\Delta\Delta H$ 2.0 kcal/mol). Low energy differences 0.4 kcal/mol for **P3-ex**/**P3-en** might suggest that under thermodynamic control, the formation of an equimolar mixture of adducts should be observed. This is, however, not the case, since for cycloadditions involving δ-lactone, the reversibility of reaction experimentally has never been observed. On the other hand, the 2.0 kcal/mol energy difference for **P1-ex**/**P1-en** of the γ-lactone might suggest the asymmetric transformation of adducts under thermodynamic control. This can be noticed since upon prolongation of the reaction time at reflux, reversibility of the cycloaddition has been observed.[33] The low stability of the nitrone caused, however, a dramatic decrease in the reaction yield, practically excluding such an asymmetric transformation. Hence, the progress of the reaction is stopped after the disappearance of substrates when the ratio of adducts, in both cases, **L1** and **L2,** is kinetically controlled.[33] Bearing this in mind, we focused attention on activation barriers and transition state structures.

The analysis of the activation enthalpies for the TSs reveals that *meta*-approaches are favored over *ortho* ones (for models involving **L1** and **L2**); this is in agreement with the FMO analysis (see Section 3.1). The **TS1-ex** and **TS1-en** (**TS3-ex** and **TS3-en**) have lower energies than **TS2-ex** and **TS2-en** (**TS4-ex** and **TS4-en**), in the range 5.0–6.5 kcal/mol (7.8–8.8 kcal/mol). This *meta*-regioselectivity is in agreement with experimental data.[34,43] The difference of activation enthalpy between *exo*- and *endo*-TSs for both channels indicates that these reactions prefer the *exo*-selectivity. However, the difference between **TS1-ex** and **TS1-en** is only 0.7 kcal/mol in comparison with the **TS3-ex**/**TS3-en** difference being equal to 3.0 kcal/mol. The activation free energies also proved this preference (deviation has been noticed for $\Delta G^{\ddagger}$ for **TS2-*ex***; this is due to the strong negative activation entropy value which is responsible for an increase of the activation free energy value).

In Table 2, the relative activation energies for reverse reactions (from adduct to reactants) have been attached. These values are close to those for direct reactions (from reactants to adduct), which indicates that both reactions involving γ- and δ-lactones are

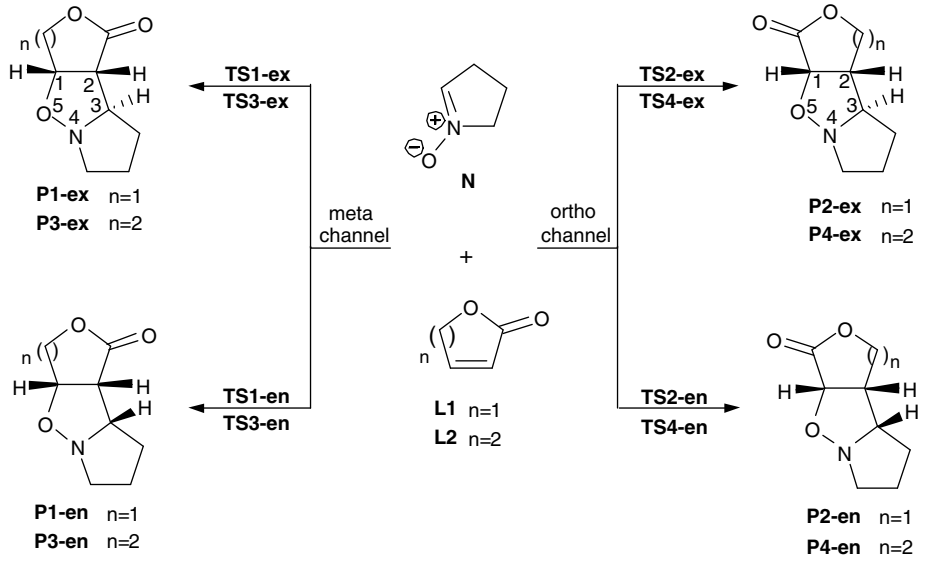

Scheme 2. The 1,3-dipolar cycloaddition reactions of nitrone **N** and lactones **L1** and **L2**.

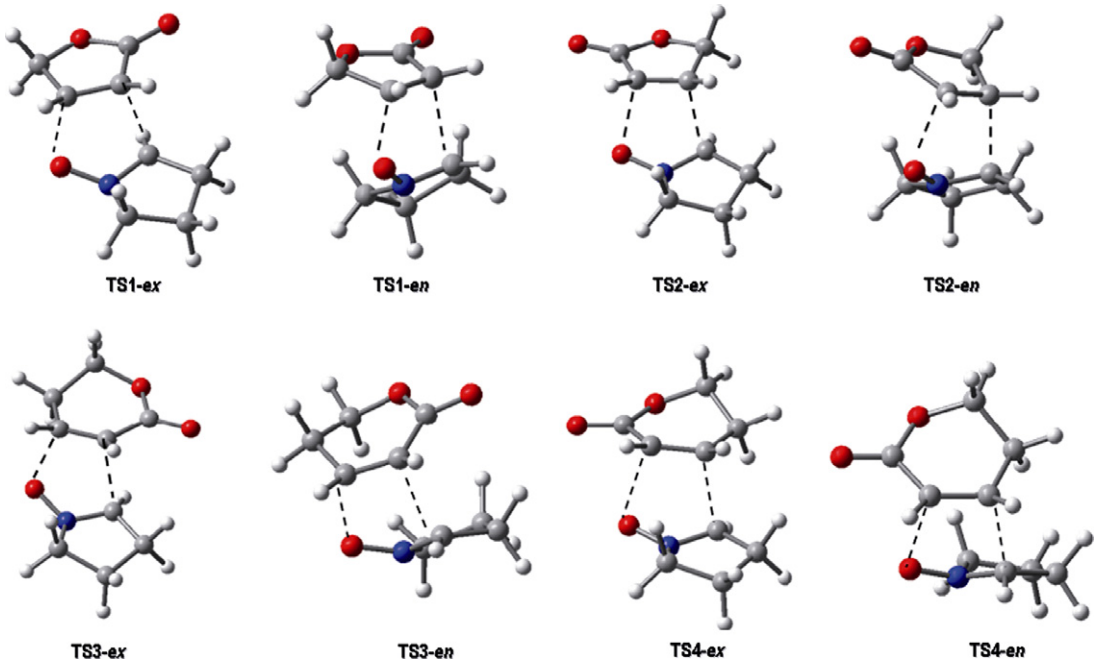

Figure 3. Transition structures for 1,3-DC reaction between the nitrone **N** and lactones **L1** and **L2**.

Table 2
Relative energies: free energies (ΔG, kcal/mol), enthalpies (ΔH, kcal/mol), and entropies (ΔS, cal/mol K) at 25 °C, for TSs and products of reaction between **N** and **L1** (**L2**)[a]

	Direct reaction			Reverse reaction		
	ΔH	ΔS	ΔG	ΔH	ΔS	ΔG
TS1-ex	18.1	−18.4	23.5	26.6	3.0	26.0
TS1-en	18.8	−19.0	24.5	25.3	0.8	25.0
TS2-ex	23.1	−23.3	30.1	27.5	3.8	26.4
TS2-en	24.6	−16.3	29.4	27.4	3.3	26.4
P1-ex	−13.2	−48.5	1.3			
P1-en	−11.2	−48.1	3.4			
P2-ex	−7.9	−48.7	6.6			
P2-en	−7.1	−47.9	7.2			
TS3-ex	19.4	−18.4	24.9	28.2	2.8	27.4
TS3-en	22.4	−16.4	27.3	29.1	3.4	29.1
TS4-ex	27.1	−16.4	31.9	30.9	3.9	29.6
TS4-en	28.2	−17.8	33.5	28.9	3.5	27.8
P3-ex	−12.9	−48.2	1.5			
P3-en	−12.5	−49.2	2.3			
P4-ex	−7.7	−20.3	6.8			
P4-en	0.0	−32.7	9.7			

[a] All TSs energies are referred to energy value of [N···L] van der Waals' molecular complex and energies of all adducts are referred to sum [N+L].

reversible. As it was mentioned above this is true for 5-membered lactone only.

To explain the experimentally observed different reactivities of γ- and δ-lactones, especially the ability of the formation of *endo*-adducts by the former and a lack of that by the latter, we analyzed the geometries of both *endo*-transition states **TS1-en** and **TS3-en**. We have found unfavorable interactions between the hydrogen atoms of the nitrone and the δ-lactone in **TS3-en** (Fig. 4). The distance between showed hydrogen atoms is 1.96 Å and this value is closed to forming bond length values (see Table 3). Similar interactions can be observed also for **TS1-en**, in this case, however, the interaction is smaller and the corresponding distance amounts to 2.60 Å. Such a disfavorable interaction in the *endo*-approach is larger for a transition state involving the 6-membered lactone which causes increase of the *endo*-TS energy (**TS3-en**), and thus consequently increases the diastereoselectivity of the reaction (strong preference of formation of the *exo*-product). On the other hand, for a reaction involving a 5-membered lactone, the steric interaction in the *endo*-approach is smaller and thus the diastereoselectivity *exo*/*endo* is lower.

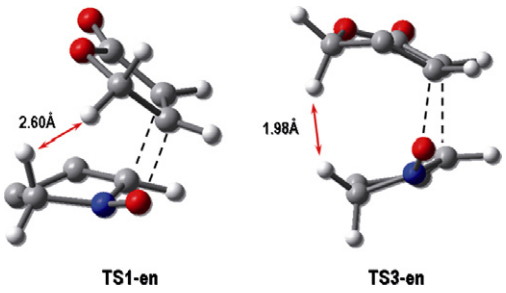

Figure 4. Geometries of both *endo*-TSs for 1,3-DCs of nitrone **N** to lactones **L1** and **L2** (some hydrogen atoms are omitted for clarity).

3.2.2. Geometrical parameters

The optimized geometries of eight TSs corresponding to the reaction of lactones **L1** and **L2** are depicted in Figure 3. The corresponding selected geometric parameters are given in Table 3.

In the case of more favorable *meta*-TSs, the lengths of the C_1–O_5 distances are shorter than for the lengths of the C_2–C_3 ones (for numbering of atoms see Scheme 2). On the other hand, the opposite is found for *ortho*-transition structures, with C_1–O_5 distances being longer than C_2–C_3 ones. Such a reverse situation is in agreement with previously studied 1,3-dipolar cycloadditions with electron-poor dipolarophiles.[28c,d] If we take into consideration that C–O bonds are more advanced than C–C bonds, the *meta* channel can be envisioned to some extent as a Michael addition (nitrone oxygen acts as a nucleophile). In one of our previous papers, bearing in mind the high preference of *anti* approach of a nitrone to the terminal substituent of the δ-lactone, we have postulated more advanced C–O bond formation.[13a] Conversely to the *meta* channel, the *ortho* one, representing a typical asynchronous process, can

Table 3
Selected geometric parameters for transition structures illustrated in Figure 3[a]

	Meta channel					*Ortho* channel			
	Atoms' distances [Å]		Dihedral angles			Atoms' distances [Å]		Dihedral angles	
	C_1–O_5	C_2–C_3	O_5–C_1–C_2–C_3	O_5–N_4–C_3–C_2		C_1–O_5	C_2–C_3	O_5–C_1–C_2–C_3	O_5–N_4–C_3–C_2
TS1-ex	1.93	2.22	5.8	48.5	**TS2-ex**	2.16	2.06	1.6	51.3
TS1-en	1.87	2.25	−1.6	−44.0	**TS2-en**	2.13	2.05	−8.6	−49.3
TS3-ex	1.95	2.20	10.2	49.3	**TS4-ex**	2.15	2.04	−2.7	49.5
TS3-en	1.92	2.20	−8.1	−43.6	**TS4-en**	2.15	2.06	−11.9	−50.6

[a] For numbering of atoms see Scheme 2.

be considered as an early TS, as it indicates a relatively long distance for the C–O bond formation.[27a]

The conformation of the isoxazolidine rings is defined by a geometry around the C_1–C_2–C_3–N_4–O_5 atoms. The results obtained are similar for both channels. All *exo*-TSs show positive values for the O_5–N_4–C_3–C_2 dihedral angle in contrast to *endo*-TSs having negative values. For both lactones larger absolute values for *ortho* channels are observed. The values of O_5–C_1–C_2–C_3 dihedral angle are in range −11.9° to 10.2°. For **TS2-ex**, **TS1-en**, and **TS4-ex**, these values are close to 0°. Such results indicate that generally these four atoms are in plane and only nitrogen atom is out-of-plane.

3.2.3. Bond orders and charge analysis

The concept of bond order (BO) can be utilized to obtain a more precise analysis of the extent of bond formation and bond breaking along the reaction pathway.[45] This theoretical tool has been used to study the molecular mechanism of chemical reactions. To follow the nature of the formation process for C_1–O_5 and C_2–C_3 bonds, the Wiberg[46] bond indexes have been computed by using the NBO population analysis as implemented in GAUSSIAN 03. The results are included in Table 4.

The general analysis of the bond order values for all the TS showed that cycloaddition reactions involving lactones are asynchronous with an interval of 0.40–0.48 and 0.36–0.64 for the *meta* and *ortho* channels, respectively. For the *meta* channel, the BOs of C_2–C_3 formation (0.40–0.43) are slightly lower than for formation of C_1–O_5 ones (0.45– 0.48). In the case of *ortho* channel, the BOs of C_2–C_3 bond formation (0.61–0.64) have greater values than for C_1–O_5 bonds (0.36–0.37). These data show a change of asynchronicity on the bond formation process for the two regioisomeric pathways.

The natural population analysis allows to evaluate the charge transfer between two reactants in the TS. The charge transfer in terms of residual charge on the nitrone fragment in TS, for all optimized TSs, is shown in Table 4. Although the positive values are indicative of an electron flow from the HOMO of the nitrone to the LUMO of the lactone, their magnitudes reveal an almost neutral reaction.

Table 4
Wiberg bond orders and charge transfer (in terms of residual charge of nitrone fragment in transition state) for transition structures **TS1-ex (TS3-ex)**, **TS1-en (TS3-en)**, **TS2-ex (TS4-ex)**, and **TS2-en (TS4-en)**[a]

	C_1–C_2	C_2–C_3	C_3–N_4	N_4–O_5	O_5–C_1	NPA q_{CT} (e)
TS1-ex	1.26	0.40	0.98	1.00	0.47	0.09
TS1-en	1.24	0.43	0.99	0.99	0.45	0.11
TS2-ex	1.26	0.61	0.94	1.07	0.36	0.17
TS2-en	1.25	0.62	0.93	1.07	0.36	0.10
TS3-ex	1.24	0.48	0.98	1.00	0.40	0.08
TS3-en	1.23	0.48	0.97	1.00	0.41	0.07
TS4-ex	1.26	0.62	0.93	1.08	0.37	0.08
TS4-en	1.25	0.64	0.92	1.07	0.36	0.04

[a] For numbering of atoms see Scheme 2.

3.3. The 1,3-DC reaction of nitrone N with ethers E1 and E2

3.3.1. Energies

The cycloaddition of nitrone **N** with ether **E1** (or **E2**) can take place along four reactive channels corresponding to the *exo*- and *endo*-approaches of reactants in two possible regioisomeric senses: the *ortho* and *meta* pathways (Scheme 3). For each nitrone–ether pair, we studied four TSs: **TS5-ex** (**TS7-ex**), **TS5-en** (**TS7-en**), **TS6-ex** (**TS8-ex**), and **TS6-en** (**TS8-en**); and four cycloadducts: **P5-ex** (**P7-ex**), **P5-en** (**P7-en**), **P6-ex** (**P8-ex**), and **P6-en** (**P8-en**).

A schematic representation of the stationary points along all reactive channels is shown in Scheme 3. Figure 5 shows the geometries of TSs corresponding to the 1,3-DC reactions involving dihydrofuran **E1** and dihydropyran **E2**, respectively, while Table 5 displays relative energies for transition states of cycloadditions for both cyclic ethers. Here again, it was assumed that the reactions proceeded from reactants [N+L] to cycloadducts via the formation of van der Waals' molecular complexes [N···L] prior to the transition state structures.[44]

From transition state structures, the related minima associated with the final cycloadducts can be obtained. All cycloaddition pathways involving dihydrofuran are exothermic processes in the range of −20.4 to −14.8 kcal/mol. The *ortho* cycloadducts **P6-ex** and **P6-en** are ca. 1.5–4.8 kcal/mol energetically more favored than the *meta* ones (**P5-ex** and **P5-en**) owing to an anomeric effect that occurs between the oxygen atom of the nitrone and the oxygen atom of the ether.[47] For both channels, a greater stability of the *exo* product than the *endo* one is predicted (ca. 0.8 and 4.1 kcal/mol for *meta* and *ortho* channels, respectively). The same tendency was predicted for reactions involving dihydropyran **E2**; the **P8-ex**/**P8-en** pair is at lower energy than the **P7-ex**/**P7-en** one and, for both channels, *exo*-adducts are more stable than *endo* ones. However, in comparison with the reaction involving **E1**, the cycloadditions involving **E2** are less exothermic (only from −12.8 to −9.8 kcal/mol), and the energy difference between both *ortho*-adduct **P8-ex**/**P8-en** is lower ($\Delta\Delta H$ only 2.7 kcal/mol) than for the **P6-ex**/**P6-en** pair ($\Delta\Delta H$ 4.1 kcal/mol).

In Table 5, the relative activation energies for reverse reactions (from adduct to reactants) have been enclosed. These values are almost two times larger than for direct reactions (from reactants to adduct) which indicates that, in contrary to reactions involving lactones, cycloadditions to both unsaturated ethers should be irreversible.

The analysis of the activation enthalpies for the TSs reveals that for both ether models,*ortho-exo*-approaches (**TS6-ex** and **TS8-ex**) are especially favored over the other ones. This is in agreement with FMO analysis (see Section 3.1) and, the formation of adducts **P6-ex** and **P8-ex** as major products has been observed.[36] Consequently, according to the experimental findings,[36] **P6-en** and **P8-en** should be minor products for reactions involving **E1** and **E2**, respectively. The calculations, however, predict energies of *meta-exo*-TSs being lower than for *ortho-endo* ones (ca. 0.7 kcal/mol for **E1** and ca. 1.9 kcal/mol for **E2**). Similar to cycloadditions to the lac-

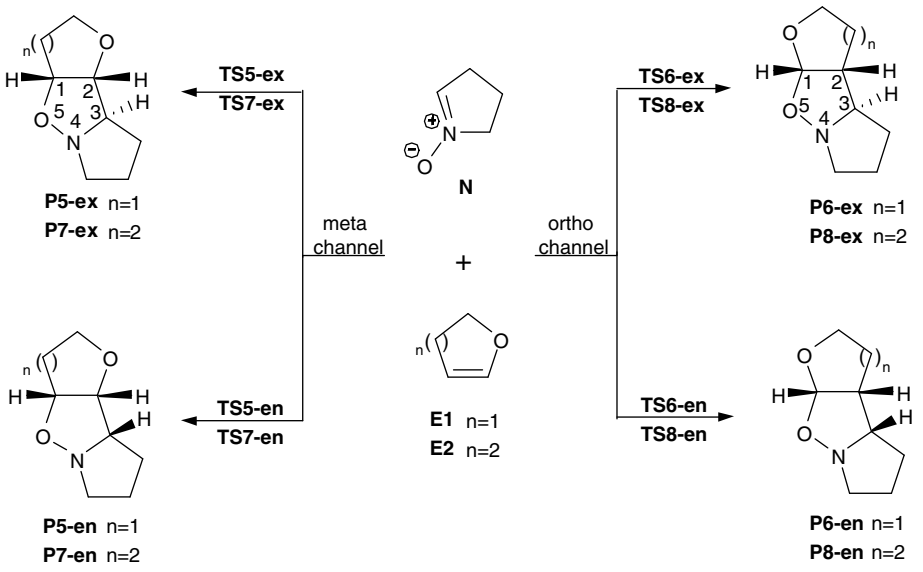

Scheme 3. The 1,3-dipolar cycloaddition reactions of nitrone **N** and ethers **E1** and **E2**.

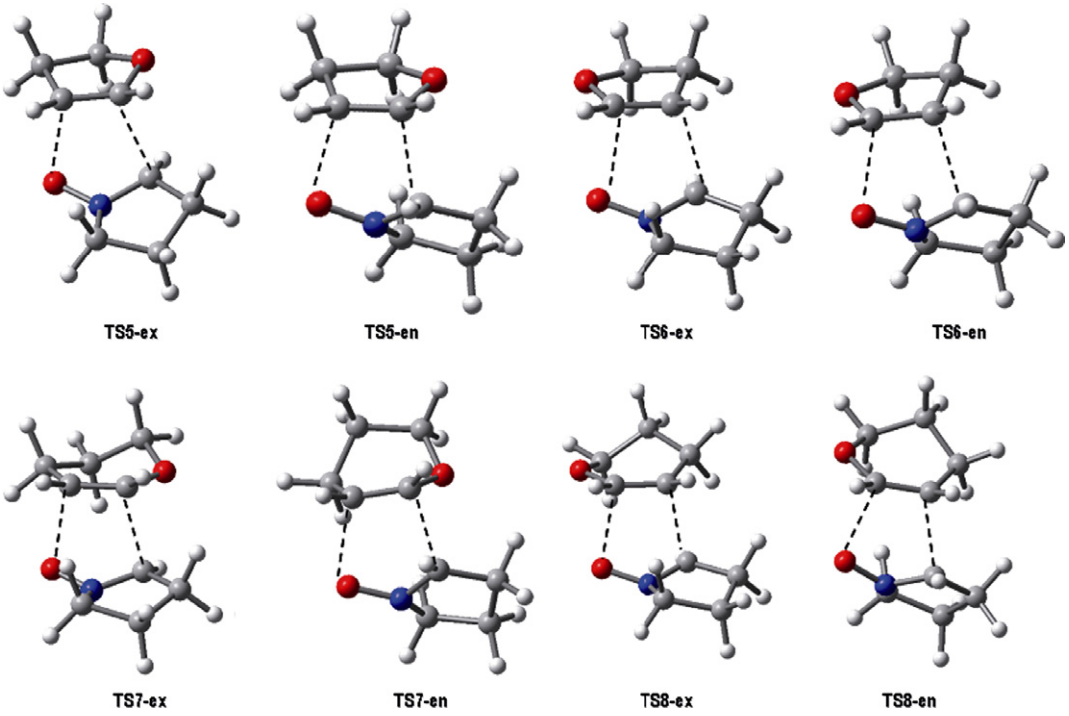

Figure 5. Transition structures for 1,3-DC reaction between the nitrone **N** and ethers **E1** and **E2**.

tones, in the case of ethers, *exo*-TSs are lower in energy than the *endo*-TSs. In contrary to the lactones TSs, however, the energy differences between *exo*- and *endo*-TSs for cycloadditions to ethers are larger. The careful analysis of geometries of two *endo*-TSs (**TS6-en** and **TS8-en**) is shown in Figure 6 (compare with Fig. 4). These *endo*-TSs are more disfavorable than corresponding lactones' ones, because of an additional hydrogen–hydrogen interaction (compare with Fig. 4).

3.3.2. Geometrical parameters and analysis of frequencies

The optimized geometries of eight TSs corresponding to the reaction of nitrone **N** with ethers **E1** and **E2** are illustrated in Figure 6. The corresponding selected geometric parameters are given in Table 6.

In the case of the more favorable *ortho*-TSs, the distances of the C_1–O_5 are slightly longer or equal to the distances of the C_2–C_3 ones (for numbering of atoms see Scheme 3). Similar results were found for 1,3-DCs to vinyl ethers.[21,27a] The opposite is found for *meta*-transition structures, with the formation of C_1–O_5 bond being less advanced than C_2–C_3 distances. However, some deviation of the general trend is found for **TS5-en**, which has a C–O forming bond longer than the C–C one.

The conformation of the isoxazolidine rings is defined by geometry around C_1–C_2–C_3–N_4–O_5 atoms. The obtained results are

Table 5
Relative energies: free energies (ΔG, kcal/mol), enthalpies (ΔH, kcal/mol), and entropies (ΔS, cal/mol K) at 25 °C, for TSs and products of reaction between **N** and **E1**(**E2**)[a]

	Direct reaction			Reverse reaction		
	ΔH	ΔS	ΔG	ΔH	ΔS	ΔG
TS5-ex	22.0	−20.0	28.0	35.6	2.7	34.8
TS5-en	24.4	−20.2	30.4	37.4	1.0	37.1
TS6-ex	19.8	−19.7	25.7	38.3	3.7	37.2
TS6-en	22.7	−20.4	28.8	37.1	3.4	36.0
P5-ex	−15.6	−49.2	−0.9			
P5-en	−14.8	−47.6	−0.6			
P6-ex	−20.4	−49.9	−5.6			
P6-en	−16.3	−46.9	−1.3			
TS7-ex	25.2	−19.6	31.1	33.9	2.1	33.3
TS7-en	29.2	−22.1	35.8	38.2	3.1	37.2
TS8-ex	22.1	−25.7	29.9	34.9	2.8	34.1
TS8-en	27.1	−19.6	33.0	36.0	0.1	35.5
P7-ex	−10.6	−47.5	3.6			
P7-en	−9.8	−47.0	4.2			
P8-ex	−12.8	−47.7	1.4			
P8-en	−10.1	−45.3	3.4			

[a] All TSs energies are referred to energy value of [N···E] van der Waals' molecular complex and energies of all adducts are referred to sum [N+E].

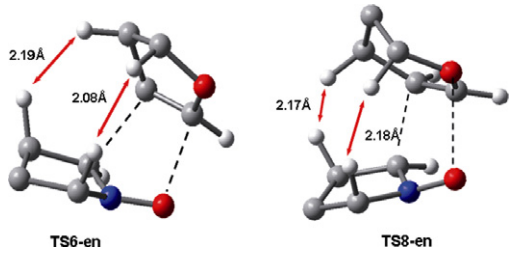

Figure 6. Geometries of both *ortho*- and *endo*-TSs for cycloadditions of nitrone **N** to ethers **E1** and **E2** (some hydrogen atoms are omitted for clarity).

similar for both channels. All *exo*-TSs show a positive value of the O_5–N_4–C_3–C_2 dihedral angle in contrast to *endo*-TSs having negative value and this is similar to trend found for lactones' TSs. Once again low value of O_5–C_1–C_2–C_3 indicates almost co-planarity of these atoms. However, positive values of dihedral angle O_5–C_1–C_2–C_3 were found for **TS-6ex** and **TS-8ex** in comparison to **TS-5ex** and **TS-7ex**. This change is probably connected with change of ether's ring size.

3.3.3. Bond orders and charge analysis

The concept of bond order (BO)[45] can be utilized to obtain more exact analysis of the extent of bond formation and bond breaking along a reaction pathway. This theoretical tool has been used to study the molecular mechanism of chemical reactions. To follow the nature of the formation process for C_1–O_5 and C_2–C_3 bonds, the Wiberg[46] bond indexes have been computed by using the NBO population analysis as implemented in GAUSSIAN 03. The results are shown in Table 7.

The general analysis of the bond order values for all the TSs showed that cycloaddition reactions involving ethers are asynchronous with an interval of 0.21–0.59 and 0.16–0.56 for the *meta* and *ortho* channels, respectively. For the *meta* channel the BOs of C_1–O_5 (0.21– 0.34) distances are slightly lower than for C_2–C_3 ones (0.26–0.59). Also in the case of the *ortho* channel, the BOs of C_2–C_3 distances (0.24–0.56) have greater values than for C_1–O_5 ones (0.16–0.31).

Finally, the natural population analysis allows us to evaluate the charge transfer between two reactants at the TS. The charge transfer in terms of residual charge on the nitrone fragment in TS, for all optimized TSs, is shown in Table 7. Although the negative values are indicative of an electron flow from the HOMO of ether to the LUMO of the nitrone, their magnitudes reveal an almost neutral reaction.

Table 7
Wiberg bond orders and charge transfer (in terms of residual charge of nitrone fragment in transition state) for transition structures **TS5-ex** (**TS7-ex**), **TS5-en** (**TS7-en**), **TS6-ex** (**TS8-ex**), and **TS6-en** (**TS8-en**)[a]

	C_1–C_2	C_2–C_3	C_3–N_4	N_4–O_5	O_5–C_1	NPA q_{CT} (e)
TS5-ex	1.32	0.58	0.95	1.05	0.34	−0.04
TS5-en	1.31	0.59	0.95	1.05	0.34	−0.06
TS6-ex	1.50	0.24	1.13	1.07	0.16	−0.05
TS6-en	1.48	0.26	1.11	1.05	0.18	−0.08
TS7-ex	1.55	0.27	1.09	1.04	0.21	−0.04
TS7-en	1.56	0.26	1.11	1.05	0.21	−0.02
TS8-ex	1.26	0.56	0.95	1.03	0.31	−0.09
TS8-en	1.47	0.27	1.11	1.06	0.18	−0.08

[a] For numbering of atoms see Scheme 3.

4. Conclusions

The presented study demonstrates that DFT calculations at B3LYP/6-31+G(d) level theory can be used for description of the cycloaddition reaction between the 5-membered cyclic nitrone and both electron-poor and electron-rich cyclic dipolarophiles. These calculations successfully reproduced experimental regio- and stereoselectivity observed by Font,[34] Kakisawa,[36] and by us,[13,32,33] although the results obtained provide only qualitative picture. According to the performed analysis, the regioselectivity (*ortho* versus *meta* channel) is controlled by FMO coefficients and/or charge distribution in reactants. Comparison of cycloadducts' and TSs' energies reveals high *exo*-diastereoselectivity for both cycloadditions, involving lactones and ethers. Moreover, theoretical results explain very well the experimentally observed differences in reactivity between 5- and 6-membered cyclic dipolarophiles. They confirm high *exo*-diastereoselectivity of cycloadditions involving latter dipolarophiles due to unfavorable steric interactions in the corresponding *endo*-transition state. Moreover, they show that these interactions are stronger for the cyclic ether than for the lactone.

Table 6
Selected geometric parameters for transition structures illustrated in Figure 5[a]

	Meta channel					*Ortho* channel			
	Atoms' distances [Å]		Dihedral angles			Atoms' distances [Å]		Dihedral angles	
	C_1–O_5	C_2–C_3	O_5–C_1–C_2–C_3	O_5–N_4–C_3–C_2		C_1–O_5	C_2–C_3	O_5–C_1–C_2–C_3	O_5–N_4–C_3–C_2
TS5-ex	2.14	2.14	−7.1	43.3	**TS6-ex**	2.21	2.17	4.6	48.9
TS5-en	2.17	2.11	−10.8	−47.7	**TS6-en**	2.17	2.17	−0.6	−45.3
TS7-ex	2.10	2.13	−4.2	43.7	**TS8-ex**	2.18	2.14	5.4	48.1
TS7-en	2.10	2.13	−9.1	−50.0	**TS8-en**	2.13	2.13	−6.6	−46.9

[a] For numbering of atoms see Scheme 3.

Our studies are the first which analyze 1,3-DC reactions involving cyclic reactants—both nitrone and dipolarophile. Consistence of theoretical predictions with experimental results put more light on such reactions and open an access to subsequent analysis of more complex cases of 1,3-DC involving reactants bearing substituents, thus introducing single or double asymmetric induction phenomena. It should be stressed that the results obtained might be helpful in planning further experiments leading to the synthesis of polyhydroxyl alkaloids having desired substitution and configuration.

Acknowledgments

Part of the calculations were performed at Department de Chimie Moleculaire (UJF, Grenoble), CIMENT/CECIC (Grenoble), and CERMAV (CNRS, Grenoble). Authors are most indebted to these centers for providing us with computer capabilities. We are also indebted to the Marie Curie Program for financial support for one of us (S.S.). Financial support for this work was provided through the Polish Ministry of Science and High Education (Grant # 3 T09A 025 28).

References

1. (a) Padwa, A. *1,3-Dipolar Cycloaddition Chemistry*; Wiley: New York, 1984; (b) Gothelf, K. V.; Jørgensen, K. A. *Chem. Rev.* **1998**, *98*, 863–909; (c) Karlsson, S.; Högberg, H.-E. *Org. Prep. Proced. Int.* **2001**, *33*, 103–172; (d) Kobayashi, S.; Jørgensen, K. A. *Cycloaddition Reactions in Organic Synthesis*; Wiley-VCH: Weinheim, 2002; (e) Pellissier, H. *Tetrahedron* **2007**, *63*, 3235–3285; (f) Padwa, A. In *Synthetic Applications of 1,3-Dipolar Cycloaddition Chemistry Toward Heterocycles and Natural Products*; Padwa, A., Pearson, W. H., Eds.; Wiley & Sons: Hoboken, NJ, 2003; (g) Merino, P.. In *Science of Synthesis*; Padwa, A., Ed.; George Thieme: New York, NY, 2004; Vol. 27, p 511; (h) Torssell, K. B. G. *Nitrile oxides, Nitrones and Nitronates in Organic Chemistry*; VCH: New York, 1998; (i) Breuer, E.; Aurich, H. G.; Nielsen, A. *Nitrones, Nitronates and Nitroxides*; Wiley: New York, 1989; (j) Confalone, P. N.; Huie, E. M. *Org. React.* **1988**, *36*, 1–174; (k) DeShong, P.; Lander, S.; Leginus, J. M.; Dicken, C. M.. In *Advanced in Cycloaddition*; Curran, D. P., Ed.; JAI Press, 1988; Vol. 1, pp 87–128; (l) Black, D.; Crozier, R. F.; Davies, V. Ch. *Synthesis* **1975**, 205–221.
2. (a) Denmark, S. E.; Thorarensen, A. *Chem. Rev.* **1996**, *96*, 137–165; (b) Denmark, S. E.; Parker, D. L.; Dixon, J. A. *J. Org. Chem.* **1997**, *62*, 435–436; (c) Denmark, S. E.; Thorarensen, A.; Middleton, D. S. *J. Am. Chem. Soc.* **1996**, *118*, 8266; (d) Denmark, S. E.; Thorarensen, A. *J. Am. Chem. Soc.* **1997**, *119*, 125–137; (e) Denmark, S. E.; Marcin, L. R. *J. Org. Chem.* **1997**, *62*, 1675–1684; (f) Denmark, S. E.; Hurd, A. R.; Sacha, H. J. *J. Org. Chem.* **1997**, *62*, 1668–1674; (g) Denmark, S. E.; Thorarensen, A. *J. Org. Chem.* **1994**, *59*, 5672–5681; (h) Denmark, S. E.; Hurd, A. R. *J. Org. Chem.* **1998**, *63*, 3045; (i) Denmark, S. E.; Hurd, A. R. *Org. Lett.* **1999**, *1*, 1311; (j) Denmark, S. E.; Hurd, A. R. *J. Org. Chem.* **2000**, *65*, 2875–2886; (k) Denmark, S. E.; Herbert, B. *J. Org. Chem.* **2000**, *65*, 2887–2896.
3. (a) Prearson, W. H. *Pure Appl. Chem.* **2002**, *74*, 1339–1347; (b) Pandey, G.; Banerjee, P.; Gadre, S. *Chem. Rev.* **2006**, *106*, 4484–4517.
4. (a) Gallos, J. K.; Koumbis, A. E. *Curr. Org. Chem.* **2003**, *7*, 397–426; (b) Gallos, J. K.; Koumbis, A. E. *Curr. Org. Chem.* **2003**, *7*, 771–797.
5. (a) Frederickson, M. *Tetrahedron* **1997**, *53*, 403–425; (b) Nair, V.; Suja, T. D. *Tetrahedron* **2007**, *63*, 12247–12275; (c) Koumbis, A. E.; Gallos, J. K. *Curr. Org. Chem.* **2003**, *7*, 585–628; (d) Broggini, G.; Zecchi, G. *Synthesis* **1999**, 905–917.
6. (a) Merino, P.; Tejero, T. *Molecules* **1999**, *4*, 169–179; (b) Revuelta, J.; Cicchi, S.; Goti, A.; Brandi, A. *Synthesis* **2007**, *4*, 485–504.
7. (a) Cicchi, S.; Goti, A.; Brandi, A. *J. Org. Chem.* **1995**, *60*, 4743–4748; (b) Goti, A.; Fedi, V.; de Sarlo, F.; Brandi, A. *Synlett* **1997**, 577–579; (c) Goti, A.; Cicchi, S.; Cacciarini, M.; Cardona, F.; Fedi, V.; Brandi, A. *Eur. J. Org. Chem.* **2000**, 3633–3645; (d) Goti, A.; Cacciarini, M.; Cardona, F.; Cordero, F.; Brandi, A. *Org. Lett.* **2001**, *3*, 1367–1369; (e) Pisaneschi, F.; Monica, C.; Cordero, F.; Brandi, A. *Tetrahedron Lett.* **2002**, *43*, 5711–5714; (f) Cordero, F.; Pisaneschi, F.; Gensini, M.; Goti, A.; Brandi, A. *Eur. J. Org. Chem.* **2002**, 1941–1951; (g) Pisaneschi, F.; Cordero, F.; Brandi, A. *Eur. J. Org. Chem.* **2003**, 4373–7375; (h) Cardona, F.; Faggi, E.; Liguori, S.; Goti, A. *Tetrahedron Lett.* **2003**, *44*, 2315–2318; (i) Cardona, F.; Moreno, G.; Guarana, F.; Vogel, P.; Schetz, C.; Merino, P.; Goti, A. *J. Org. Chem.* **2005**, *70*, 6552–6555; (j) Pisaneschi, F.; Piacenti, M.; Cordero, F.; Brandi, A. *Tetrahedron: Asymmetry* **2006**, *17*, 292–296.
8. Carmona, A. T.; Whigtman, R. H.; Robina, I.; Vogel, P. *Helv. Chim. Acta* **2003**, *86*, 3066–3073.
9. (a) McCraig, A.; Meldrum, K. P.; Whigtman, R. H. *Tetrahedron* **1998**, *54*, 9429–9446; (b) Hull, A.; Meldrum, K. P.; Therand, P. R.; Whigtman, R. H. *Synlett* **1997**, 123–125.
10. Peer, A.; Vasella, A. *Helv. Chim. Acta* **1999**, *82*, 1044–1065.
11. Kuban, J.; Kolarovic, A.; Fisera, L.; Jager, V.; Humpa, O.; Pronayova, N. *Synlett* **2001**, *12*, 1866–1868.
12. (a) Socha, D.; Jurczak, M.; Chmielewski, M. *Carbohydr. Res.* **2001**, *336*, 315–318; (b) Socha, D.; Paśniczek, K.; Jurczak, M.; Solecka, J.; Chmielewski, M. *Carbohydr. Res.* **2006**, *341*, 2005–2011; (c) Paśniczek, K.; Socha, D.; Solecka, J.; Jurczak, M.; Chmielewski, M. *Can. J. Chem.* **2006**, *84*, 534–539; (d) Panfil, I.; Solecka, J.; Chmielewski, M. *J. Carbohydr. Chem.* **2006**, *25*, 673–684; (e) Paśniczek, K.; Solecka, J.; Chmielewski, M. *J. Carbohydr. Chem.* **2007**, *26*, 195–211; (f) Panfil, I.; Urbańczyk-Lipkowska, Z.; Chmielewski, M. *Pol. J. Chem.* **2005**, *79*, 239–249.
13. (a) Paśniczek, K.; Socha, D.; Jurczak, M.; Frelek, J.; Suszczyńska, A.; Urbańczyk-Lipkowska, Z.; Chmielewski, M. *J. Carbohydr. Chem.* **2003**, *22*, 613–629; (b) Socha, D.; Jurczak, M.; Frelek, J.; Klimek, A.; Rabiczko, J.; Urbańczyk-Lipkowska, Z.; Suwińska, K.; Chmielewski, M.; Cardona, F.; Goti, A.; Brandi, A. *Tetrahedron: Asymmetry* **2001**, *12*, 3163–3172; (c) Jurczak, M.; Rabiczko, J.; Socha, D.; Chmielewski, M.; Cardona, F.; Goti, A.; Brandi, A. *Tetrahedron: Asymmetry* **2000**, *11*, 2015–2022.
14. (a) Overman, L. E.; Taylor, G. F.; Houk, K. N.; Domelsmith, L. N. *J. Am. Chem. Soc.* **1978**, *100*, 3182–3191; (b) Bimanand, A. Z.; Gupta, Y. N.; Doa, M. J.; Eaton, T. A.; Houk, K. N.; Fronczek, F. R. *J. Org. Chem.* **1983**, *48*, 403–413; (c) Vedejs, E.; Perry, D. A.; Houk, K. N.; Rondan, N. G. *J. Am. Chem. Soc.* **1983**, *105*, 6999–7005; (d) Houk, K. N.; Lin, Y.-T.; Brown, F. K. *J. Am. Chem. Soc.* **1986**, *108*, 554–561; (e) Curran, D. P.; Kim, B. H.; Piyasena, H. P.; Loncharich, R. J.; Houk, K. N. *J. Org. Chem.* **1987**, *52*, 2137–2143; (f) Brown, F. K.; Houk, K. N.; Burnell, D. J.; Valenta, Z. *J. Org. Chem.* **1987**, *52*, 3051–3060; (g) Raimondi, L.; Brown, F. K.; Gonzalez, J.; Houk, K. N. *J. Am. Chem. Soc.* **1992**, *114*, 4796; (h) Brown, F. K.; Chandra Singh, U.; Kollman, P. A.; Raimondi, L.; Houk, K. N.; Bock, C. W. *J. Org. Chem.* **1992**, *57*, 4862–4869; (i) Houk, K. N.; Gonzalez, J.; Li, Y. *Acc. Chem. Res.* **1995**, *28*, 81–90; (j) Goldstein, E.; Beno, B.; Houk, K. N.; Loncharich, R. J.; Brown, F. K. *J. Am. Chem. Soc.* **1996**, *118*, 6036–6043; (k) Jones, G. O.; Guner, V. A.; Houk, K. N. *J. Phys. Chem. A* **2006**, *110*, 1216–1224; (l) Silvero, G.; Lucero, M. J.; Winterfeldt, E.; Houk, K. N. *Tetrahedron* **1998**, *54*, 7293–7300.
15. Sauer, J.; Sustmann, R. *Angew. Chem., Int. Ed. Engl.* **1980**, *19*, 778–807.
16. (a) Alves, C. N.; de Silva, A. B. F.; Mati, A.; Moliner, V.; Oliva, M.; Andres, J.; Domingo, L. R. *Tetrahedron* **1997**, *58*, 2695–2700; (b) Domingo, L. R.; Picher, M. T.; Aurell, J. *J. Phys. Chem. A* **1999**, *103*, 11425–11430; (c) Oliva, M.; Andres, J.; Domingo, L. R. *THEOCHEM* **2001**, *544*, 79–90; (d) Domingo, L. R.; Aurell, M. *J. Org. Chem.* **2002**, *67*, 959–965; (e) Domingo, L. R.; Aurell, M.; Perez, P.; Contreras, R. *J. Org. Chem.* **2003**, *68*, 3884–3890; (f) Arroyo, P.; Picher, M.; Domingo, L. R.; Terrier, F. *Tetrahedron* **2005**, *61*, 7359–7365; (g) Alvas, C. N.; Carneiro, A. S.; Andres, J.; Domingo, L. R. *Tetrahedron* **2006**, *62*, 5502–5509; (h) Berski, S.; Andreas, J.; Silvi, B.; Domingo, L. R. *J. Phys. Chem. A* **2006**, *110*, 13939–13947; (i) Domingo, L. R.; Aurell, M.; Arno, M.; Saey, J. A. *J. Org. Chem.* **2007**, *72*, 4220–4227.
17. Tanaka, K.; Imase, T.; Iwata, S. *Bull. Chem. Soc. Jpn.* **1996**, *69*, 2243–2248.
18. Herrera, R.; Nagarajan, A.; Morales, M.; Mendez, F.; Jimenez-Vazquez, H.-A.; Gerardo Zepeda, J.; Tamiaz, J. *J. Org. Chem.* **2001**, *66*, 1252–1264.
19. Silva, M.; Goldman, J. M. *Tetrahedron* **2002**, *58*, 3667–3672.
20. Raimondi, L. *Gazz. Chim. Ital.* **1997**, *127*, 167–175.
21. Liu, J.; Niwayama, S.; You, Y.; Houk, K. N. *J. Org. Chem.* **1998**, *63*, 1064–1073.
22. Yeung, M. L.; Li, W. K.; Liu, H. J.; Wang, Y.; Chan, K. S. *J. Org. Chem.* **1998**, *63*, 7670–7673.
23. (a) Ochiai, M.; Obayashi, M.; Morita, K. *Tetrahedron* **1967**, *23*, 2641–2650; (b) Winterfeldt, E.; Krohn, W. *Angew. Chem., Int. Ed. Engl.* **1967**, *6*, 709–715; (c) Lablanche-Combier, A.; Villaume, M. L. *Tetrahedron* **1968**, *24*, 6951–6958; (d) Grigg, R.; Jordan, M.; Tangthongkum, A. *J. Chem. Soc., Perkin Trans. 1* **1984**, 47–57; (e) Dalgard, N. K. A.; Larsen, K. E.; Torssell, K. B. G. *Acta Chim. Scand. B* **1984**, *38*, 423–431; (f) Panfil, I.; Belzecki, C.; Chmielewski, M.; Suwińska, K. *Tetrahedron* **1989**, *45*, 233–238.
24. Magnuson, E. C.; Pranata, J. *J. Comput. Chem.* **1998**, *19*, 1795–1804.
25. Mendez, F.; Tamariz, J.; Geerlings, P. *J. Phys. Chem. A* **1998**, *102*, 6292–6296.
26. Cossío, F. P.; Morao, I.; Jiao, H.; Schleyer, P. *J. Am. Chem. Soc.* **1999**, *121*, 6737–6746.
27. (a) Domingo, L. R. *Eur. J. Org. Chem.* **2000**, 2273–2284; (b) Carda, M.; Portoles, P.; Murga, J.; Uriel, S.; Marco, J. A.; Domingo, L. R.; Zaragoza, R.; Röper, H. *J. Org. Chem.* **2000**, *65*, 7000–7009; (c) Aurell, M.; Domingo, L. R.; Perez, P.; Conreras, R. *Tetrahedron* **2004**, *60*, 11503–11509.
28. (a) Merino, P.; Anoro, S.; Merchan, F. L.; Tejero, T. *Heterocycles* **2000**, *53*, 861–869; (b) Merino, P.; Mates, J. A.; Revuelta, J.; Tejero, T.; Chiacchio, U.; Romeo, G.; Iannazze, D.; Romeo, R. *Tetrahedron: Asymmetry* **2002**, *13*, 173–190; (c) Merino, P.; Revualta, J.; Tejero, T.; Chiacchio, U.; Rescifina, A.; Romeo, G. *Tetrahedron* **2003**, *59*, 3581–3592; (d) Merino, P.; Tejero, T.; Chiaccio, U.; Romeo, G.; Rescifina, A. *Tetrahedron* **2007**, *63*, 1448–1458.
29. Kouklovsky, C.; Dirat, O.; Berranger, T.; Langlois, Y.; Tam-Huu-Dau, M. E.; Riche, C. *J. Org. Chem.* **1998**, *63*, 5123–5128.
30. Milet, A.; Gimbert, Y.; Greene, A. E. *J. Comput. Chem.* **2006**, *27*, 157–162.
31. (a) Di Valentin, C.; Freccero, M.; Gandolfi, R.; Rastelli, A. *J. Org. Chem.* **2000**, *65*, 6112–6120; (b) Rastelli, A.; Gandolfi, R.; Sarzi-Amande, M.; Carboni, B. *J. Org. Chem.* **2001**, *66*, 2449–2458.
32. Stecko, S.; Paśniczek, K.; Jurczak, M.; Urbańczyk-Lipkowska, Z.; Chmielewski, M. *Tetrahedron: Asymmetry* **2006**, *17*, 68–79.
33. Stecko, S.; Paśniczek, K.; Jurczak, M.; Urbańczyk-Lipkowska, Z.; Chmielewski, M. *Tetrahedron: Asymmetry* **2007**, *18*, 1085–1093.
34. (a) Cid, P.; de March, P.; Figueredo, M.; Font, J.; Milan, S. *Tetrahedron Lett.* **1992**, *33*, 667–670; (b) Alonso-Perarnau, D.; de March, P.; Figueredo, M.; Font, J.; Soria, A. *Tetrahedron* **1993**, *49*, 4267–4274.
35. (a) Cardona, F.; Valenza, S.; Goti, A.; Brandi, A. *Tetrahedron Lett.* **1997**, *38*, 8097–8100; (b) Cardona, F.; Valenza, S.; Picasso, S.; Goti, A.; Brandi, A. *J. Org. Chem.* **1998**, *63*, 7311–7318; (c) Cardona, F.; Sałański, P.; Chmielewski, M.; Valenza, S.; Goti, A.; Brandi, A. *Synlett* **1999**, 1444–1446.

36. (a) Iwashita, T.; Kusumi, T.; Kakisawa, H. *Chem. Lett.* **1979**, 1337–1340; (b) Kakisawa, H.; Iwashita, T.; Kusumi, T. *J. Org. Chem.* **1982**, *47*, 230–233.
37. Frisch, M. J.; Trucks, G. W.; Schlegel, H. B.; Scuseria, G. E.; Robb, M. A.; Cheeseman, J. R.; Montgomery, Jr., J. A.; Vreven, T.; Kudin, K. N.; Burant, J. C.; Millam, J. M.; Iyengar, S. S.; Tomasi, J.; Barone, V.; Mennucci, B.; Cossi, M.; Scalmani, G.; Rega, N.; Petersson, G. A.; Nakatsuji, H.; Hada, M.; Ehara, M.; Toyota, K.; Fukuda, R.; Hasegawa, J.; Ishida, M.; Nakajima, T.; Honda, Y.; Kitao, O.; Nakai, H.; Klene, M.; Li, X.; Knox, J. E.; Hratchian, H. P.; Cross, J. B.; Bakken, V.; Adamo, C.; Jaramillo, J.; Gomperts, R.; Stratmann, R. E.; Yazyev, O.; Austin, A. J.; Cammi, R.; Pomelli, C.; Ochterski, J. W.; Ayala, P. Y.; Morokuma, K.; Voth, G. A.; Salvador, P.; Dannenberg, J. J.; Zakrzewski, V. G.; Dapprich, S.; Daniels, A. D.; Strain, M. C.; Farkas, O.; Malick, D. K.; Rabuck, A. D.; Raghavachari, K.; Foresman, J. B.; Ortiz, J. V.; Cui, Q.; Baboul, A. G.; Clifford, S.; Cioslowski, J.; Stefanov, B. B.; Liu, G.; Liashenko, A.; Piskorz, P.; Komaromi, I.; Martin, R. L.; Fox, D. J.; Keith, T.; Al-Laham, M. A.; Peng, C. Y.; Nanayakkara, A.; Challacombe, M.; Gill, P. M. W.; Johnson, B.; Chen, W.; Wong, M. W.; Gonzalez, C.; Pople, J. A. GAUSSIAN 03, Revision B.04; Gaussian, Pittsburgh, PA, 2003.
38. (a) Becke, A. D. *J. Chem. Phys.* **1993**, *98*, 5648–5652; (b) Becke, A. D. *Phys. Rev. A* **1988**, *38*, 3098–3100; (c) Lee, C.; Yang, W.; Parr, R. G. *Phys. Rev. B* **1988**, *37*, 785–789.
39. Schlegel, H. B. Geometry Optimization on Potential Energy Surface. In *Modern Electronic Structure Theory*; Yarkony, D. R., Ed.; World Scientific Publishing: Singapore, 1994.
40. Reed, A. E.; Weinstock, R. B.; Weinhold, F. *J. Chem. Phys.* **1985**, *83*, 735–746.
41. (a) Fukui, K. *Acc. Chem. Res.* **1981**, *14*, 363–368; (b) Head-Gordon, M.; Pople, J. A. *J. Chem. Phys.* **1988**, *89*, 5777–5786.
42. Mayo, P.; Hecnar, T.; Tam, W. *Tetrahedron* **2001**, *57*, 5931–5941.
43. (a) Tufariello, J.; Tette, J. *J. Org. Chem.* **1975**, *40*, 3866–3869; (b) Tufariello, J. *Acc. Chem. Res.* **1979**, *12*, 396–403.
44. Sustmann, R.; Sicking, R.; Huisgen, W. *J. Am. Chem. Soc.* **1995**, *117*, 9679–9685.
45. Reed, A. E.; Curtiss, L.; Weinhold, F. *Chem. Rev.* **1988**, *88*, 899–926.
46. Wiberg, K. *Tetrahedron* **1968**, *24*, 1083–1096.
47. Perrin, C. L.; Armstrong, K. G.; Fabian, M. A. *J. Am. Chem. Soc.* **1994**, *116*, 715–722.